Liquid Crystals

DOI: 10.1002/ange.201408438

Supramolecular [60]Fullerene Liquid Crystals Formed By Self-Organized Two-Dimensional Crystals**

Xiaoyan Zhang, Chih-Hao Hsu, Xiangkui Ren, Yan Gu, Bo Song, Hao-Jan Sun, Shuang Yang, Erqiang Chen, Yingfeng Tu, Xiaohong Li, Xiaoming Yang, Yaowen Li, and Xiulin Zhu**

Abstract: *Fullerene-based liquid crystalline materials have both the excellent optical and electrical properties of fullerene and the self-organization and external-field-responsive properties of liquid crystals (LCs). Herein, we demonstrate a new family of thermotropic [60]fullerene supramolecular LCs with hierarchical structures. The [60]fullerene dyads undergo self-organization driven by π–π interactions to form triple-layer two-dimensional (2D) fullerene crystals sandwiched between layers of alkyl chains. The lamellar packing of 2D crystals gives rise to the formation of supramolecular LCs. This design strategy should be applicable to other molecules and lead to an enlarged family of 2D crystals and supramolecular liquid crystals.*

The discovery of graphene and other two-dimensional (2D) crystals has shown that 2D crystals can be stable at room temperature.[1] The covalent bonds between the atoms in these 2D crystals are key, holding the atoms in the crystal lattice and suppressing thermal fluctuations.[2] Herein, we report that π–π interactions, which are considered as weak intermolecular forces comparable to hydrogen-bond interactions,[3] can also drive the formation of 2D crystals in a properly designed system of fullerene derivatives. Furthermore, the lamellar packing of 2D crystals forms a new family of thermotropic supramolecular liquid crystals (LCs) with hierarchical structures.

The structure of the [60]fullerene derivatives used herein is shown in Figure 1a. A typical molecule from these dyads consists of a rigid [60]fullerene, a gallic ester segment

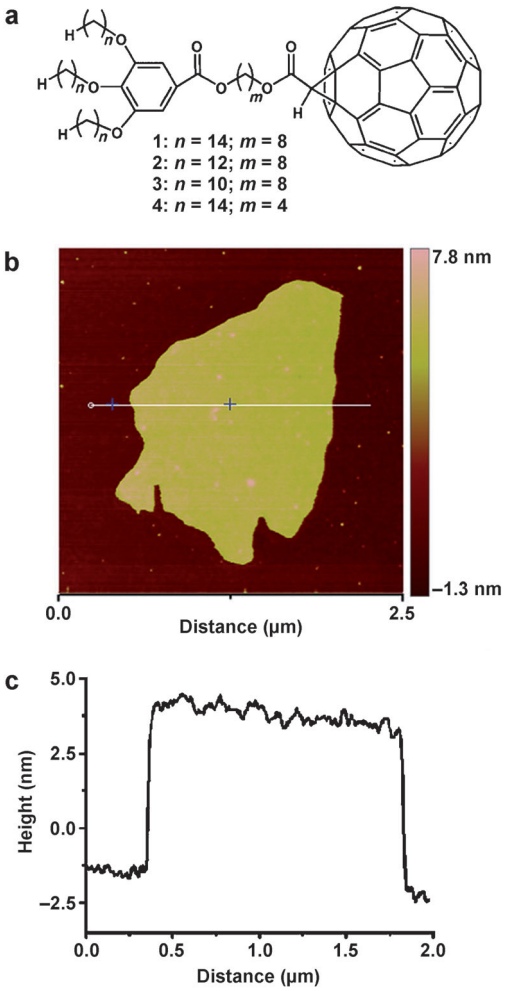

Figure 1. a) Molecular structure of fullerene dyads **1**–**4**. b) The AFM image of 2D crystals formed by dyad **1**. c) The height profile at the cross-section indicated in (b).

substituted with three long alkyl chains as the soft part, and a multi-methylene unit as a flexible spacer connecting the two segments. Detailed synthetic routes and characterization of the samples can be found in Figures S1–S3 in the Supporting Information. The design strategy here is to introduce a soft group onto fullerene (considered as the rigid component) so the molecules will self-organize to form supramolecules as

[*] X. Zhang,[+] Y. Gu, Prof. B. Song, Prof. Y. Tu, Prof. X. Li, Prof. X. Yang, Prof. Y. Li, Prof. X. Zhu
Jiangsu Key Laboratory of Advanced Functional Polymer Design and Application, College of Chemistry
Chemical Engineering and Materials Science
Soochow University, Suzhou 215123 (P.R. China)
E-mail: tuyingfeng@suda.edu.cn
xlzhu@suda.edu.cn
Dr. C.-H. Hsu,[+] Dr. H.-J. Sun
College of Polymer Science and Polymer Engineering
The University of Akron, Akron, OH 44325 (USA)
Dr. X. Ren, Prof. S. Yang, Prof. E. Chen
Department of Polymer Science and Engineering
College of Chemistry and Molecular Engineering
Peking University, Beijing 100871 (P.R. China)
[+] These authors contributed equally to this work.

[**] We gratefully acknowledge financial support from the National Natural Science Foundation of China (Grant No. 21074079, 21274099), and a Project Funded by the Priority Academic Program Development of Jiangsu Higher Education.

Supporting information for this article is available on the WWW under http://dx.doi.org/10.1002/anie.201408438.

a result of π–π interactions between fullerenes and phase separation between the rigid and the soft parts. The soft groups form continuous lamellar layers above and below the fullerene layers to form 2D crystals. In other words, the dyad molecules form a sandwiched structure with the fullerene units in the middle layer, which is similar to the lamellar phase separation of block copolymers.[4]

Compounds **1**–**3** can form 2D crystals upon evaporation of solvent from their corresponding dilute solutions. In contrast, **4** does not form 2D crystals under these conditions. Figures 1 b and c show the AFM image and corresponding height profile for the crystals formed by sample **1**. The corresponding images for samples **2** and **3** can be found in Figures S4 and S5. Free-standing flat crystals are clearly evident with a lateral size of several microns and a layer thickness of 5–6 nm. As the crystal thickness along the *c* axis is only several nanometers and a few molecules thick and much smaller than the length of the crystal along the *ab* plane (several microns), they can be regarded as 2D crystals.[1]

The formation of 2D crystals is further confirmed by TEM measurements. Figure 2 a shows the bright-field image of **2**. The layers with different shades of gray from light to dark indicate different layers of 2D crystals. The selected area electron diffraction pattern from a monolayer film of 2D crystals is shown in the inset in Figure 2 a (the assignment of the diffraction spots can be found in Figure S6). The diffraction spot pattern indicates that the fullerenes are packed in a quadrate motif in the crystal lattice with distance to adjacent fullerenes of approximately 1.01 nm, measured by comparing the pattern with the diffraction spots obtained from a standard sample (TlCl). This value is same as the distance between adjacent fullerenes in typical [60]fullerene crystals (1.00 nm),[5] indicating that the driving force for the formation of 2D crystals is π-π interactions between fullerenes. This assignment is supported by the red shift of bands in the UV/Vis absorption spectra of the dyads′ film compared to the corresponding bands in the spectra recorded from the solution (Figure S7). The tilting experiments also reveal the face-centered orthorhombic packing of fullerenes in the subunit cell with $a = b = 1.43$ nm and $c' = 1.7$ nm (Figure S8).

A bulk sample of **2** was sheared, microtomed, and directly imaged by TEM to reveal the structures along the *c* direction (perpendicular to the 2D crystal plane). As shown in Figure 2 b, well-ordered lamellar structures were observed with an average distance between the layers of approximately 5 nm, in agreement with the results obtained from AFM. The fullerene-rich part is dark in color as a result of its high electron density, whereas the gray part corresponds to the alkyl chains. The width of the dark line is about 2–3 nm, corresponding to the fullerene layer thickness along the *c*′ axis in the 2D crystals with a sandwich structure. This distance is larger than that measured in a double-layer packing structure (ca. 2.0 nm) which was reported in some fullerene derivative-containing self-assembled supramolecules.[6] The layer thickness demonstrates the triple-layer packing structure of fullerenes along the *c* axis in the 2D crystals, which is confirmed by tilting electron diffraction experiments and density measurements (see the Supporting Information).

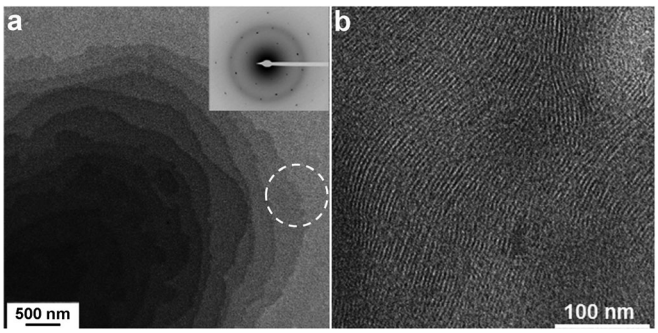

Figure 2. TEM images of the 2D crystals formed by dyad **2**. a) Bright-field image of 2D crystals measured perpendicular to the layers. Inset: electron diffraction pattern from selected monolayer 2D crystals (white circle). b) Bright-field cross-section image of microtomed layer-by-layer stacked 2D crystals.

Interestingly, stacking of 2D crystals in the bulk forms LCs at room temperature and at higher temperatures. Figure 3 a shows the thermotropic phase behavior of dyads **1**–**4** measured by differential scanning calorimetry (DSC; see Figure S9 for curves). Dyads **1**–**3** can form liquid crystalline phases with particular liquid crystalline textures observed by polarized optical microscopy (POM; Figure 3 b for dyad **2**, Figures S10 and S11 for others). The fact that dyad **4** cannot form a liquid crystalline phase indicates that the formation of 2D crystals is critical to the subsequent formation of a thermotropic LC. For sample **1**–**3**, the first transition below room temperature corresponds to the melting of alkyl chains (crystal to LC phase transition), with the second transition corresponding to the LC to isotropic transition. The enthalpies for the LC to isotropic transition of samples are very similar (ca. 8.0 kJ mol^{-1}) despite different alkyl-chain lengths. This coincides well with our previous observation that the driving force for the formation of 2D crystals is π–π interactions between fullerenes.

The packing structure of dyad molecules **1**–**3** in the LC state is studied by small-angle X-ray scattering (SAXS). The SAXS data for sample **2** is presented in Figure 3 c, with the corresponding Miller indices (*h k l*) given in parentheses on top of the peak. The SAXS data for the other samples are presented in Figure S12 and S13. All three samples show similar diffraction patterns but different peak positions because of different lamella thicknesses. The first peak (at $2\theta = 1.54°$, corresponding to a *d* spacing of 5.73 nm) and the accompanying higher order peaks up to (*0 0 7*) suggest that there is a well-ordered lamella structure in the LC state. The measured *d* spacing indicates the distance between 2D crystals and is in good agreement with the data obtained from AFM and TEM measurements. Wide-angle X-ray diffraction (WAXD; Figure S14) reveals there is another set of peaks which follows the diffraction rules for a face-centered orthorhombic structure (all odd or even numbers of indices). This result further demonstrates the triple-layer crystalline packing of fullerenes in the 2D crystals when combining the results from electron diffraction experiments. The indices denoted using a ′ symbol indicate the Miller indices along the *c*′ axis in the subunit of 2D fullerene crystals. The assignment

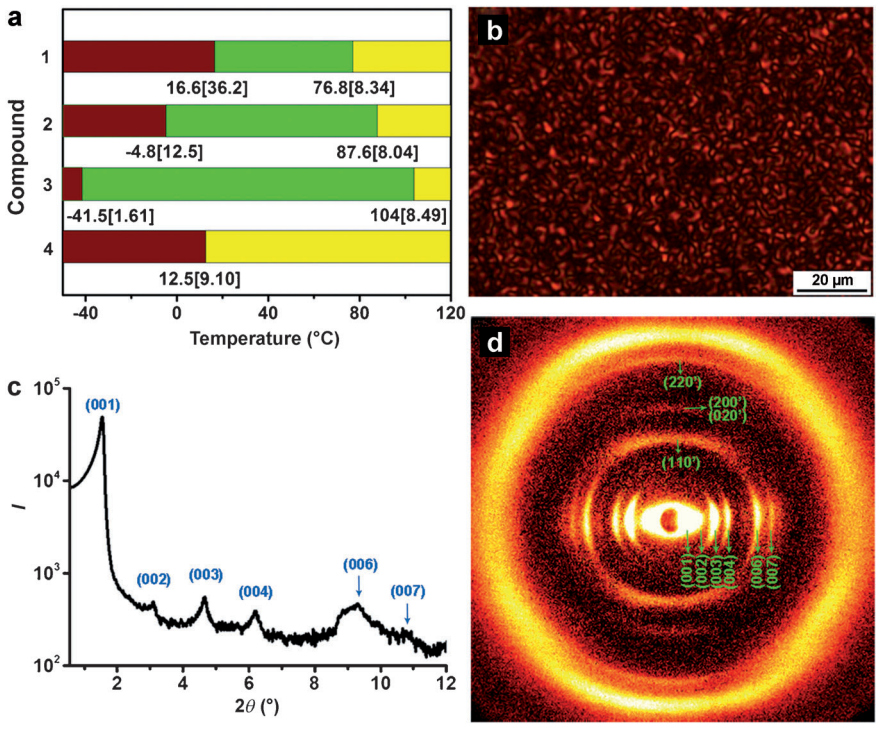

Figure 3. The bulk properties of dyads **1**–**4**. a) Thermotropic phase behavior of **1**–**4**. Deep red = crystalline phase; green = liquid-crystalline phase; yellow = isotropic phase. The numbers within the plot indicate temperature (°C), with transition enthalpies (kJ mol^{-1}) given in square brackets. b) POM image of **2** at room temperature. c) The full SAXS spectrum of **2** at 30 °C. d) 2D WAXD pattern of the sheared bulk sample of **2**. The incident X-ray beam is perpendicular to the shear direction and parallel to the 2D crystal planes.

of these peaks is confirmed by the 2D WAXD from sheared samples (Figure 3 d and Figure S15). In Figure 3 d, where the incident beam is parallel to the LC smectic and 2D crystal planes, the strong arcs at the equator indicate the well-ordered lamella structure of the LCs. At the meridian position, the inner arcs can be assigned to the diffraction resulting from 2D fullerene subunit crystals. Note, even in the sheared sample, only 2D crystals which have fullerenes at the suitable position (i.e. the diffraction plane parallel to the incident beam) can give the corresponding diffraction peaks. This is why the signals at meridian are much weaker compared to the equator.

When the incident beam is perpendicular to the lamella layer (along the *c* axis), no diffraction spot or arc is detected, but instead circles are detected by 2D WAXD (Figure S15). On the other hand, electron diffraction from stacked lamellae of 2D crystals gives different sets of quadrate diffraction spots from corresponding 2D crystals. The results suggest that there is no correlation between different 2D crystals, that is, the isotropic molten alkyl-chain layers make the 2D crystals stack freely.

The molecular packing of dyad **2** in the supramolecular LCs with hierarchical structure is illustrated in Figure 4. The

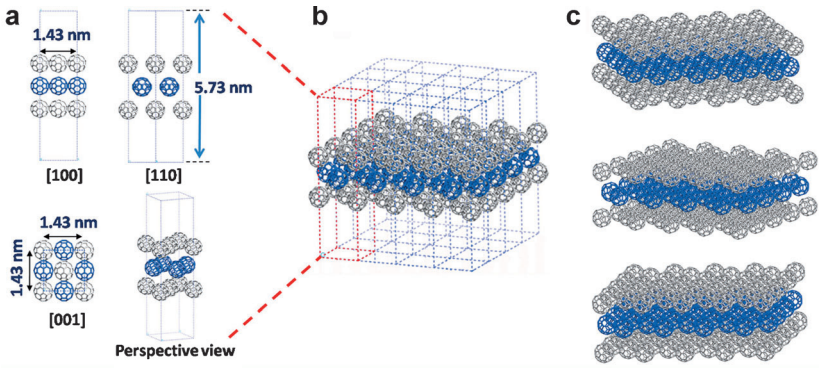

Figure 4. Representation of molecular packing of dyad **2** into 2D crystals and LCs, with the alkyl chains omitted for clarity. a) The triple-layer fullerene packing in a LC lattice observed from different aspects. b) The triple-layer subunit fullerene 2D crystals in the LC lattices. c) The supramolecular LCs formed by the free stacking of 2D crystals.

LC lattice belongs to the orthogonal crystal system with $a = b = 1.43$ nm, $c = 5.73$ nm, and six molecules in a unit cell (Figure 4 a and b). The packing of lamellae forms the supramolecular LCs (Figure 4 c). Within the LC lamella, the crystalline fullerene layers form the 2D crystals along the *ab* plane, sandwiched between the alkyl-chain double layers, with a triple-layer face-centered orthorhombic subunit cell structure ($a = b =$ 1.43 nm and $c' = 1.72$ nm, c' is the z axis of the subunit of 2D fullerene crystals, and is parallel to the c axis of the liquid-crystal lattice). Considering only the fullerene balls, the fullerenes in the second layer are positioned at the top of the holes formed by the quadrate packing of fullerenes in the first layer. For fullerenes in the middle layer, the flexible spacers penetrate from the quadrate-packing holes so the alkyl chains are in the soft part of the layer. This type of structure has not been previously reported. The packing structure explains why the fullerenes choose in-plane quadrate packing but not hexagonal packing, because the diameter of the holes formed by the quadrate packing (0.41 nm) is much larger than hexagonal packing (0.15 nm), thus the flexible spacer can penetrate from the middle layer. This is supported by the fact that dyad **4** cannot form 2D crystals as a result of its shorter flexible spacer length.

These are the first reported thermotropic LCs formed by 2D crystals. By definition, these LCs are smectic LCs, but with long-range positional order of the fullerene moieties within the lamella. The LCs belong to the family of supramolecular

fullerene LCs[7] with hierarchical structure, where the dyad molecules self-organize to form triple-layer 2D crystals and the free lamella packing of 2D crystals forms supramolecular LCs. In this regard, these are supramolecular liquid crystals formed by 2D crystals.

The formation method of these thermotropic liquid crystals is somewhat like the inorganic platelets formed lyotropic LCs,[8] where the crystalline montmorillonite platelets were dispersed in water and formed a nematic phase at concentrations higher than a critical volume predicted by Onsager.[8a] Gabriel et al. reported long-range positional lamellar order for their aqueous solid-acid platelets which formed lyotropic LCs, together with long-range 2D atomic positional order within the platelets.[8d] Recently, aqueous solutions of graphene oxide were also shown to have lyotropic LC properties, where a graphene monolayer can be considered as a large 2D crystal.[9] In our case, the alkyl chains are in a molten state and act like solvent molecules to disperse the triple-layer 2D crystals. As a result of the covalent linkage of alkyl chains with the fullerenes, they form soft lamellar layers sandwiching the triple-layer 2D crystals. It should be noted that there is no correlation between 2D crystals at different LC lamellae because of the free motion of the alkyl chains. This is critical for the formation of LC phases as it destroys the positional ordering between lamellae and hinders the formation of crystals.

The principle outlined herein should be applicable to design and obtain other types of supramolecular LCs with hierarchical structures formed from the self-organization of 2D crystals. As fullerenes are part of the LC mesogen, these supramolecular LCs have a high fullerene content. Consequently, the LCs should display the excellent optoelectronic properties of fullerenes and at the same time the liquid crystalline nature should give rise to external stimuli responsive properties.

Received: August 21, 2014
Published online: October 19, 2014

Keywords: fullerenes · liquid crystals · π interactions · self-assembly · X-ray diffraction

[1] a) K. S. Novoselov, A. K. Geim, S. V. Morozov, D. Jiang, Y. Zhang, S. V. Dubonos, I. V. Grigorieva, A. A. Firsov, *Science* **2004**, *306*, 666 – 609; b) K. S. Novoselov, D. Jiang, F. Schedin, T. J. Booth, V. V. Khotkevich, S. V. Morozov, A. K. Geim, *Proc. Natl. Acad. Sci. USA* **2005**, *102*, 10451 – 10453; c) A. H. Castro Neto, K. Novoselov, *Mater. Express* **2011**, *1*, 10 – 17.

[2] a) N. D. Mermin, H. Wagner, *Phys. Rev. Lett.* **1966**, *17*, 1133 – 1136; b) N. D. Mermin, *Phys. Rev.* **1968**, *176*, 250 – 254.

[3] J. Alper, *Science* **2002**, *295*, 2396 – 2397.

[4] a) L. Leibler, *Macromolecules* **1980**, *13*, 1602 – 1617; b) I. W. Hamley, *The Physics of Block Copolymers*, Oxford University Press, Oxford, **1998**.

[5] a) W. Krätschmer, L. D. Lamb, K. Fostiropoulos, D. R. Huffman, *Nature* **1990**, *347*, 354 – 358; b) Y. Guo, N. Karasawa, W. A. Goddard, *Nature* **1991**, *351*, 464 – 467.

[6] a) S. Campidelli, E. Vázquez, D. Milic, M. Prato, J. Barberá, D. M. Guldi, M. Marcaccio, D. Paolucci, F. Paolucci, R. Deschenaux, *J. Mater. Chem.* **2004**, *14*, 1266 – 1272; b) W.-S. Li, Y. Yamamoto, T. Fukushima, A. Saeki, S. Seki, S. Tagawa, H. Masunaga, S. Sasaki, M. Takata, T. Aida, *J. Am. Chem. Soc.* **2008**, *130*, 8886 – 8887; c) J. Vergara, J. Barberá, J. L. Serrano, M. B. Ros, N. Sebastián, R. de La Fuente, D. O. López, G. Fernández, L. Sánchez, N. Martín, *Angew. Chem. Int. Ed.* **2011**, *50*, 12523 – 12528; *Angew. Chem.* **2011**, *123*, 12731 – 12736; d) H.-J. Sun, Y. Tu, C.-L. Wang, R. M. Van Horn, C.-C. Tsai, M. J. Graham, B. Sun, B. Lotz, W.-B. Zhang, S. Z. D. Cheng, *J. Mater. Chem.* **2011**, *21*, 14240 – 14247.

[7] a) M. Sawamura, K. Kawai, Y. Matsuo, K. Kanie, T. Kato, E. Nakamura, *Nature* **2002**, *419*, 702 – 705; b) I. M. Saez, J. W. Gooby, *J. Mater. Chem.* **2005**, *15*, 26 – 40; c) Y.-W. Zhong, Y. Matsuo, E. Nakamura, *J. Am. Chem. Soc.* **2007**, *129*, 3052 – 3053; d) J. Lenoble, S. Campidelli, N. Maringa, B. Donnio, D. Guillon, N. Yevlampieva, R. Deschenaux, *J. Am. Chem. Soc.* **2007**, *129*, 9941 – 9952; e) T. Nakanishi, Y. Shen, J. Wang, S. Yagai, M. Funahashi, T. Kato, P. Fernandes, H. Móhwald, D. G. Kurth, *J. Am. Chem. Soc.* **2008**, *130*, 9236 – 9237.

[8] a) L. Onsager, *Ann. N. Y. Acad. Sci.* **1949**, *51*, 627 – 659; b) G. J. Vroege, H. N. W. Lekkerkerker, *Rep. Prog. Phys.* **1992**, *55*, 1241 – 1309; c) J.-C. P. Gabriel, P. Davidson, *Adv. Mater.* **2000**, *12*, 9 – 20; d) J.-C. P. Gabriel, F. Camerel, B. J. Lemaire, H. Desvaux, P. Davidson, P. Batail, *Nature* **2001**, *413*, 504 – 508; e) N. Miyamoto, H. Iijima, H. Ohkubo, Y. Yamauchi, *Chem. Commun.* **2010**, *46*, 4166 – 4168; f) M. A. Bizeto, A. L. Shiguihara, V. R. L. Constantino, *J. Mater. Chem.* **2009**, *19*, 2512 – 2525; g) F. M. van der Kooij, H. N. W. Lekkerkerker, *J. Phys. Chem. B* **1998**, *102*, 7829 – 7832.

[9] a) J. E. Kim, T. H. Han, S. H. Lee, J. Y. Kim, C. W. Ahn, J. M. Yun, S. O. Kim, *Angew. Chem. Int. Ed.* **2011**, *50*, 3043 – 3047; *Angew. Chem.* **2011**, *123*, 3099 – 3103; b) Z. Xu, C. Gao, *ACS Nano* **2011**, *5*, 2908 – 2915; c) X. Yang, C. Guo, L. Ji, Y. Li, Y. Tu, *Langmuir* **2013**, *29*, 8103 – 8107.

